



# **EFFECTS OF HIGH-FREQUENCY EARTHQUAKES ON NUCLEAR POWER PLANTS USING SOIL-STRUCTURE INTERACTION ANALYSIS**

**Hyunsung Park<sup>1</sup>, Gilyoung Chung<sup>2</sup>, Soohyuk Chang<sup>3</sup>**

<sup>1</sup> General Manager, CENITS Corporation Inc., Seoul, South Korea (parkhs0328@gmail.com)

<sup>2</sup> Senior Manager, CENITS Corporation Inc., Seoul, South Korea (cgy0201@nate.com)

<sup>3</sup> President, CENITS Corporation Inc., Seoul, South Korea (rndceo68@naver.com)

## **ABSTRACT**

This study performed seismic analysis considering Soil-Structure Interaction (SSI) targeting a containment building and an auxiliary building of a nuclear power plant (NPP) in operation to understand the effect of a high-frequency earthquake that exceeds the designed limit to a NPP. The analysis was performed using two seismic waves with different frequency characteristics to identify the influence of high-frequency earthquakes. The first is a regular seismic wave corresponding to the design response spectrum of the Regulation Guide 1.60 (RG 1.60). The other is a high-frequency seismic wave corresponding to the Uniform Hazard Spectrum (UHS) made by the Probabilistic Seismic Hazard Analysis (PSHA) of the Uljin region in Korea. Seismic analysis considering SSI was performed using seismic waves with two types of frequency characteristics and analyzed the effect of a high-frequency seismic wave taking three-dimensional directional component combination, soil properties, and seismic wave incoherency effect into account.

## **INTRODUCTION**

The 2016 earthquake in Gyeongju, Korea, had a characteristic that is different from the design response spectrum of RG 1.60 and exceeded the RG 1.60's design response spectrum at a high-frequency component over 10Hz. In general, seismic waves with high-frequency characteristics have a more significant effect on safety-related devices with high natural frequencies compared to structures with a low natural frequency. Since such safety-related devices are located on several floors of a NPP, seismic analysis of the structures must be performed for an accurate seismic resistance performance examination.

SSI was taken into consideration for the seismic analysis of the structure. SSI analysis is a physical phenomenon where soil and structure affect each other and is performed in specific areas such as a precision seismic analysis of socially important structures such as massive infrastructures, skyscrapers, and NPPs. The United States of America began to apply SSI on earthquake resistance design in its NPPs in the 1970s, and it became a common practice in Korea to consider SSI for seismic analysis of safety-related facilities of NPPs in the 2000s. The Standard Review Plan 3.7.2 (SRP 3.7.2), revised by the U.S. Nuclear Regulatory Commission (US-NRC), strictly requires to consider SSI for earthquake analysis of all safety-related facilities built under the soil's shear-wave velocity under 8,000ft/s.

Based on such regulations, the effects of a high-frequency earthquake on the structural response of the NPP were studied by comparing the structural response of high-frequency seismic waves and regular seismic waves with SSI analysis. In addition, SSI analysis was performed based on three-dimensional component combinations, soil properties, and seismic wave incoherency effect. Then the results were compared and analyzed.

## PARAMETERS OF THE STUDY

### Structure

Among the NPP, the Reactor Containment Building (RCB) and the Auxiliary Building (AB) were modeled (Figure 1), and the response of the AB, where safety-related devices such as motor control center, battery charger, and switchgear were mainly reviewed in this paper. The model was improved to reflect the torsional behavior caused by the three-dimensional effect and the positional characteristics of the floor equipment in the existing single-node analysis model for each floor. The analysis model was made based on a solid element for the foundation and backfill, a plate element for the in-between of backfill and structure, and a beam element with a concentrated mass for the RCB and AB.

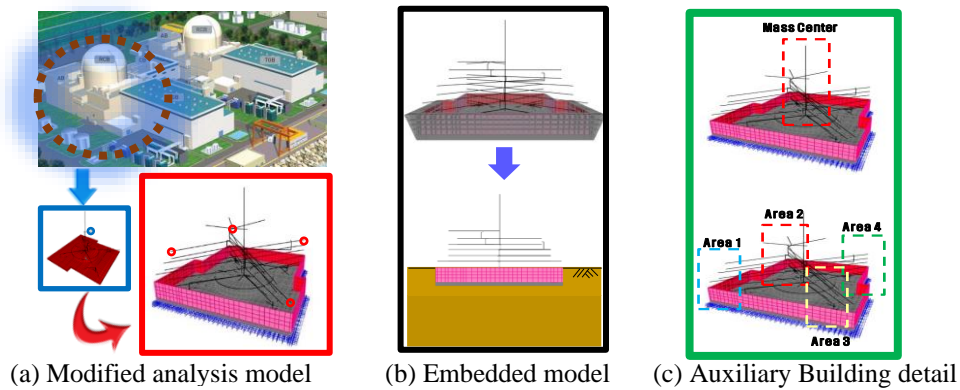


Figure 1. Analysis model of Nuclear Power Plant

### Input earthquake

For seismic analysis, two seismic waves with different frequency characteristics were used. The first is a seismic wave with general characteristics (hereinafter referred to as RG 1.60 wave), a seismic wave that conforms to the design response spectrum of RG 1.60, and the independent seismic waves in each direction (three-direction five sets, a total of fifteen waves) were used for analysis. The other seismic wave with high-frequency characteristics (hereinafter referred to as UHS wave) is a seismic wave that conforms to UHS created through the PSHA of Uljin, Korea, and an independent seismic wave in each direction (three-direction five sets, a total of fifteen waves) were used for analysis.

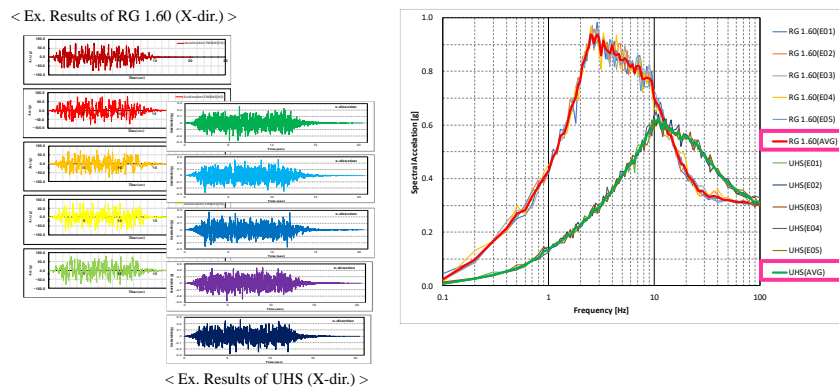


Figure 2. Seismic waves based on RG 1.60 and UHS

### THREE-DIMENSIONAL EFFECT BASED ON THE COMBINATION OF DIRECTION COMPONENT

According to the regulations required for seismic analysis, it is specified that when considering the three components of an earthquake that are statistically independent, the final response should be obtained by algebraically summing each independent response at every time interval. Following the above rule, SSI analysis was performed for each direction, and the three-dimensional direction component results were derived by summing each independent response for each time interval. The analysis was performed assuming a homogeneous soil to exclude variability due to the soil. At the center of mass and the outer location (Area 1 to 4), the response spectrum in which the three-way component was combined and the one-way response spectrum in which the direction component was not combined were compared for the UHS wave and the RG 1.60 wave. The horizontal direction analysis result is shown in Figure 3, and the vertical direction analysis result is as shown in Figure 4. For numerical comparison of the response spectrum with three-direction components combined (3D-RS) and the one-direction response spectrum (1D-RS), the variance of the response spectrum was calculated using Equation (1). The horizontal direction variance is shown in Figure 5, and the vertical direction variance is shown in Figure 6.

$$e^{(RS)} = \frac{\int_0^f \max(S_a^{(1D-RS)}(f) - S_a^{(3D-RS)}(f)) df}{\int_0^f \max S_a^{(1D-RS)}(f) df} \quad (1)$$

According to the horizontal direction variance based on locations of structure shown in Figure 5, the variance of the Area 1 to 4 has shown a more significant increase than the variance from the center of the mass. In addition, the variance in a high-frequency region ( $\geq 10$  Hz) was significantly increased compared to the low-frequency region ( $< 10$  Hz). Comparing the variance of seismic waves with different frequency characteristics, the variance between the RG 1.60 waves and the UHS waves in the low-frequency region was similar, but in a high-frequency region, the variance of the UHS wave increased significantly compared to the variance of the RG 1.60 wave. Due to the influence of the torsional mode of the AB, it is judged that the response of a high-frequency region of 10 Hz or more is greatly affected when a high-frequency characteristic earthquake is applied.

Looking at the vertical direction variance based on the structure location shown in Figure 6 no significant difference is displayed as the variance from the center of the mass is within 1%, but the variance at the Area 1 to 4 has increased significantly. When comparing earthquakes that hold different frequency characteristics, RG 1.60 wave shows a similar increase of variance in both low and high-frequency ranges, but the UHS wave shows a higher increase in variance at low-frequency than at high-frequency. It is believed that this is because of the characteristics analysis model in which the horizontal bending deformation of the AB influences the vertical displacement of the Area 1 to 4.

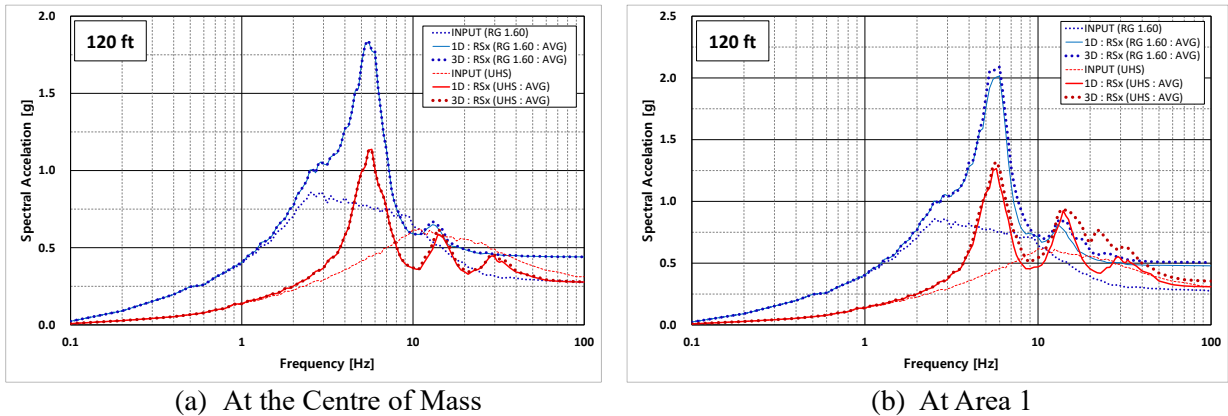


Figure 3. Comparison of ISRS for Three-Dimensional Effect (Horizontal direction, 120 ft, Damping 5%)

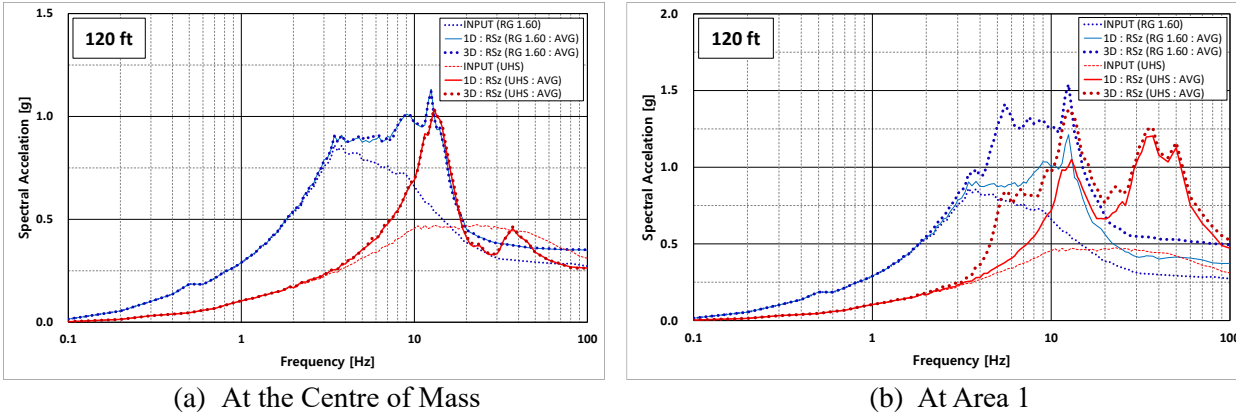


Figure 4. Comparison of ISRS for Three-Dimensional Effect (Vertical direction, 120 ft, Damping 5%)

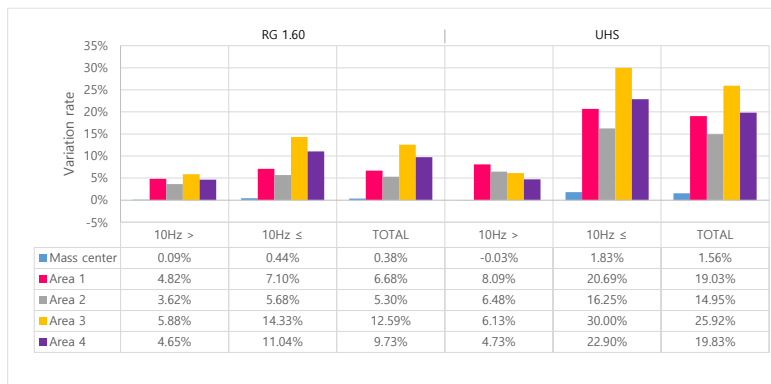


Figure 5. Comparison of variance for Three-Dimensional Effect (Horizontal direction, 120 ft)

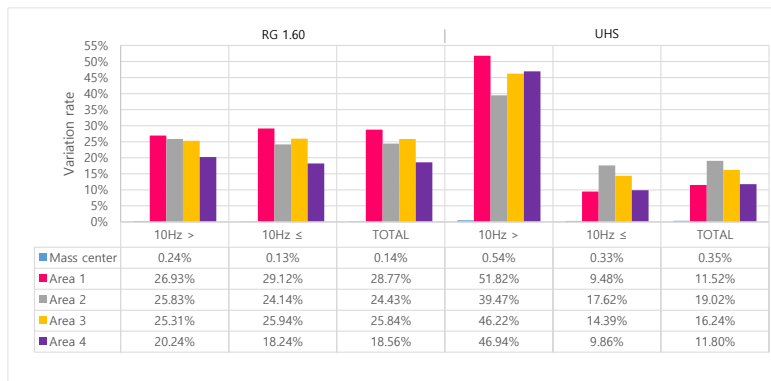


Figure 6. Comparison of variance for Three-Dimensional Effect (Vertical direction, 120 ft)

## CHANGE IN SOIL PROPERTIES

Among the nine generic soil profiles inclusions suggested by the US-NRC S4, S7, and S9 soil, which carries similar characteristics to that of NPPs sites in Korea, were compared through SSI analysis to study the structure response based on the change of soil properties. The shear wave velocity was modified in consideration of the frequency of analysis, and the element size of the analysis model for the selected soil properties and the shear wave velocity by depth is shown in Figure 7.

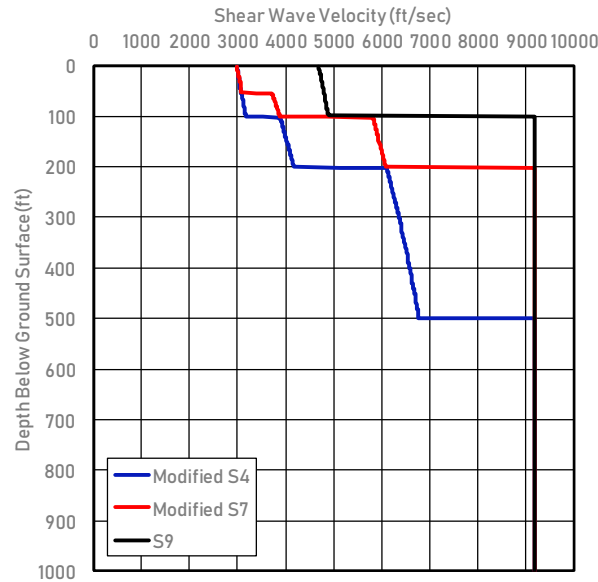


Figure 7. Soil Properties

The horizontal response spectrum based on the soil for each input earthquake is presented in Figure 8 and Figure 9. Figure 10 shows the calculation based on the variance according to the soil change of the horizontal direction In-Structure Response Spectrum (ISRS) at the center of mass and the Area 1 to 4 to understand the effect that the UHS wave and the RG 1.60 wave can have on the soil. Looking at the variance in the horizontal direction, in all the S4, S7, and S9 soils, the variance was higher in the low-frequency region below 10 Hz compared to the variance in a high-frequency region of 10 Hz or higher.

The vertical response spectrum according to the soil for each input earthquake is presented in Figure 11 and Figure 12. Figure 13 represents the assessment that is done on the ISRS from the center of mass and Area 1 to 4 based on the variance due to soil change to understand the effect that the UHS wave and the RG 1.60 wave can bring to the soil. Looking into the vertical direction variance, overall, the S7 and S9 soil response increased compared to S4 soil, similar to the result of the horizontal direction.

Regardless of the frequency characteristics of the input earthquake in both the horizontal and vertical directions, the harder the ground, the greater the response of the structure.

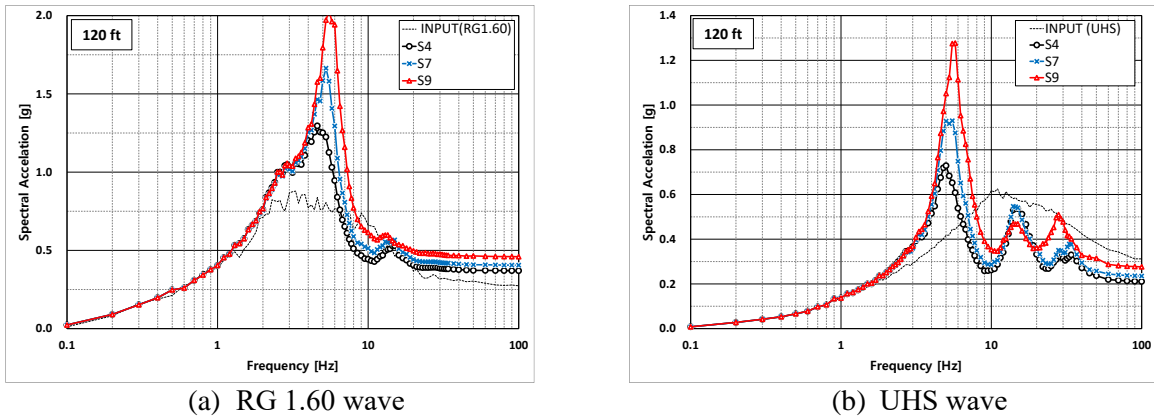


Figure 8. Comparison of ISRS for soil properties (Horizontal direction, mass center, 120 ft, Damping 5%)

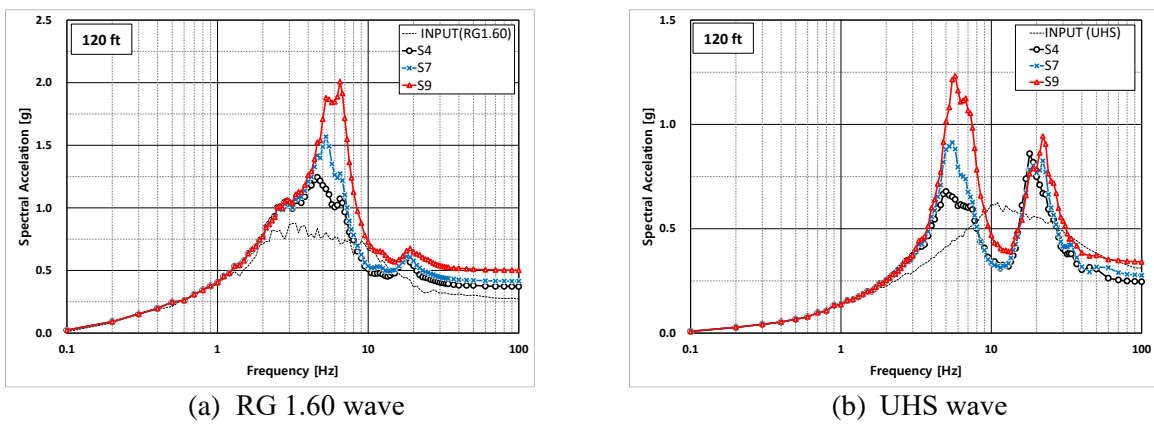


Fig. 9. Comparison of ISRS for Soil Properties (Horizontal direction, Area 3, 120 ft, Damping 5%)

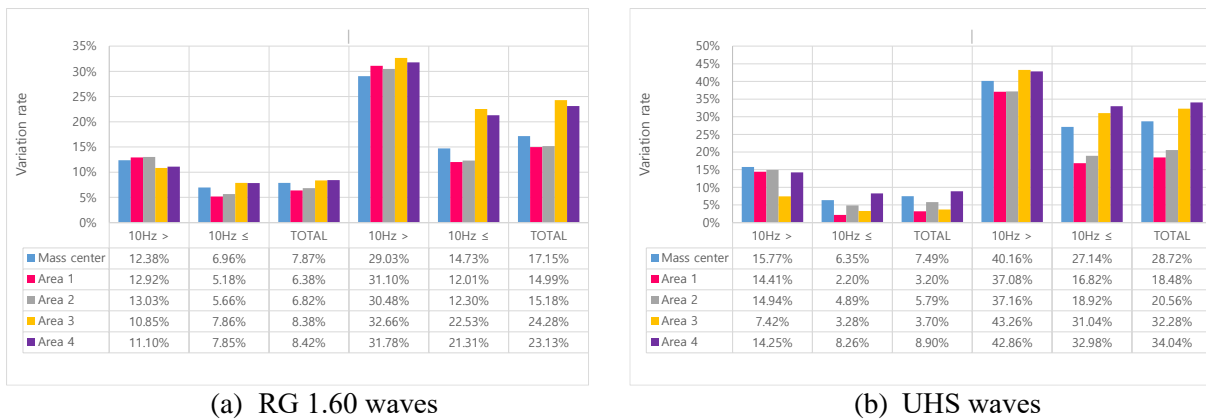


Figure 10. Comparison of variance for Soil properties (Horizontal direction, 120 ft)

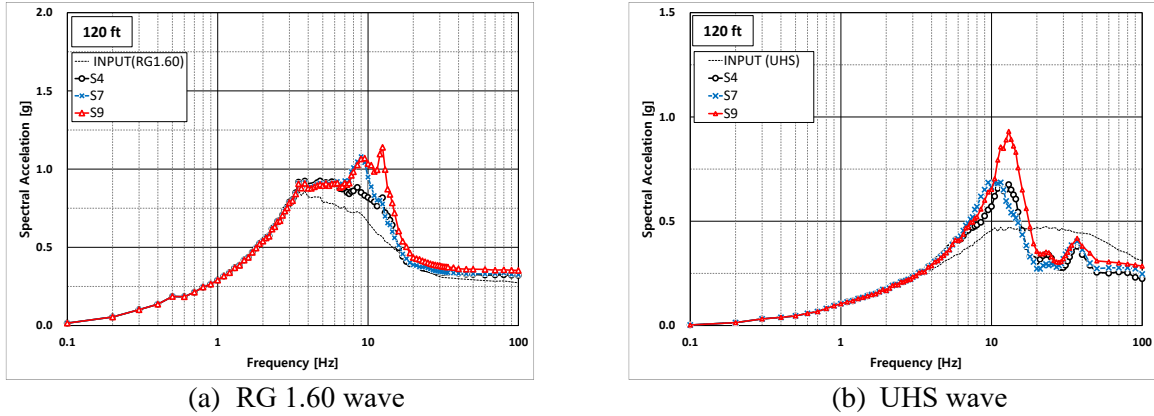


Figure 11. Comparison of ISRS for Soil Properties (Vertical Direction, mass center, 120 ft, Damping 5%)

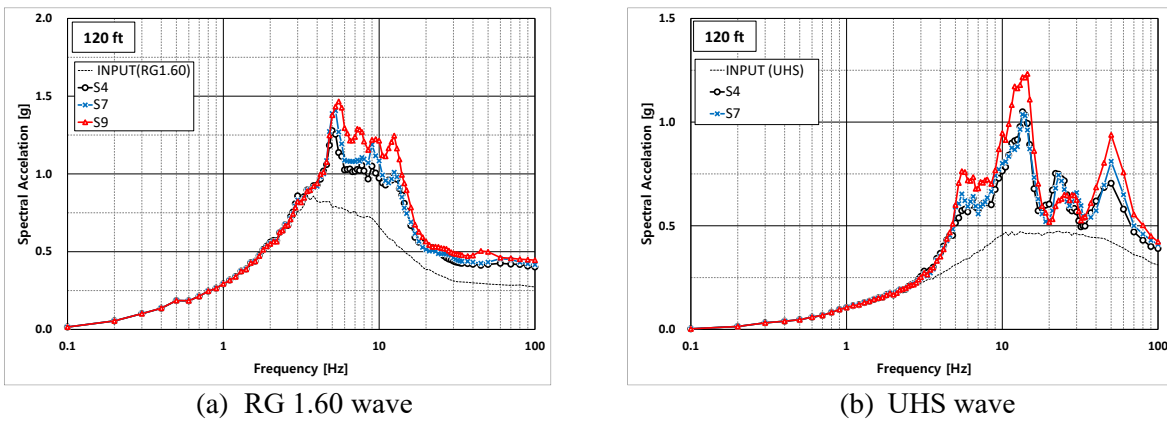


Figure 12. Comparison of ISRS for Soil Properties (Vertical Direction, Area 3, 120 ft, Damping 5%)

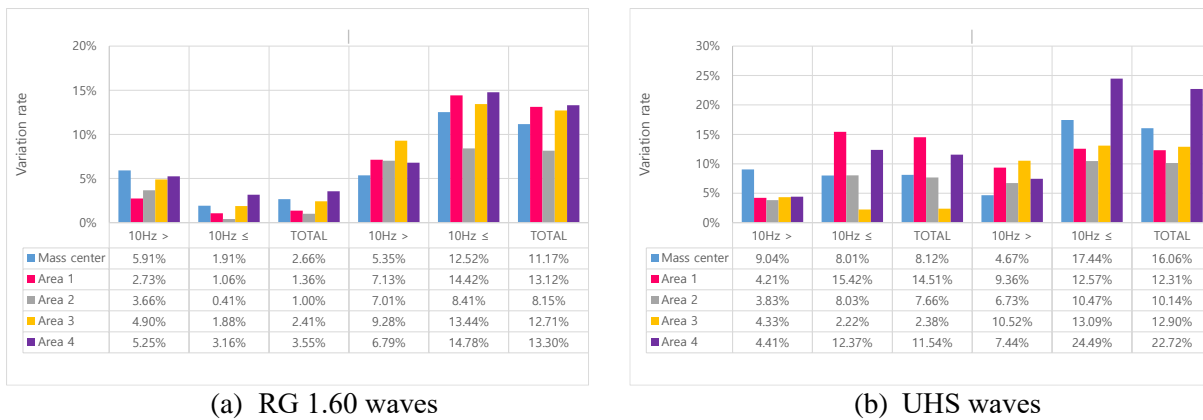


Figure 13. Comparison of Variation rate for Soil properties (Vertical direction, 120 ft)



## SEISMIC WAVE INCOHERENCY EFFECTS

Seismic wave incoherence arises from the horizontal spatial variation of both horizontal and vertical ground motions. Generally, the incoherency effects reduce the foundation translational motions and increase the rotational motions. Meanwhile, the response decreases as the size of the analyzed structure are significant and the natural frequency is high, or the input earthquake has characteristics of a high-frequency band. SSI analysis considering the seismic wave incoherency effect was performed to understand such behavior, and the process was carried out using Luco & Mita (1987) and Abrahamson (Hard Rock, 2007) models provided by SASSI2010. The analysis was performed with the soil subject for analysis assumed to be homogenous soil to exclude the variability of the analyzed soil. The following is a brief explanation of the coherence model used in the analysis.

### *Luco & Mita's coherency model*

Luco and Mita (1987) proposed an idealized coherency function where the foundation system is assumed to massless circular basemat and subjected to spatially incoherent horizontal and vertical ground motion inputs, and the responses of the foundation in terms of the translational and rotational (torsional or rocking) response transfer. Luco & Mita's coherence function model shows the form of the exponential function as follows Equation (2).

$$\gamma_{ij}(r, \omega) = \exp \left\{ - \left[ \frac{\gamma_{w} |\bar{r}_j - \bar{r}_i|}{V_s} \right]^2 \right\} \quad (2)$$

Where  $\omega$  is the circular frequency (rad/sec),  $r$  is the linear distance between two points,  $\gamma$  is the dimensionless spatial incoherence parameter, and  $V_s$  is the shear wave coherence rate. The distance  $(\bar{r}_j - \bar{r}_i)$  is the measure of separation of two points in the ground. As shown in Equation (2), for short separation and low frequency, coherency function approaches one.

### *Abrahamson's coherency model*

The hard rock coherency model is developed using only the Pinyon Flat array data (hard rock site), this model has been approved for application for nuclear power plant structures by US-NRC. This model expressed using  $\tanh(a_3\xi)$  to satisfy correlation 1 when the separation distance is zero. The hard rock coherency function is expressed by the following Equation (3).

$$\gamma_{PW}(f, \xi) = \left[ 1 + \left( \frac{f \tanh(a_3\xi)}{a_1 f_c(\xi)} \right)^{n1(\xi)} \right]^{-1/2} \left[ 1 + \left( \frac{f \tanh(a_3\xi)}{a_2} \right)^{n2} \right]^{-1/2} \quad (3)$$

Where  $\gamma_{PW}$  is the plane wave coherency representing random horizontal spatial variation of ground motion,  $f$  is ground motion frequency (Hz), and  $\xi$  is the separation distance between locations in meters. Parameters appropriate for a rock site are defined in Table 1. The model coefficients were derived from data from 80 earthquakes recorded by the Pinyon Flat array. These earthquakes were selected from 287 events, based on good signals in the frequency range of 10 Hz to 40 Hz.

Figure 14 shows the horizontal response spectrum per location calculated by averaging the responses of five sets for each direction combining the direction components. Variance is presented using the difference in the range of response spectrum of each of the analysis results to effectively compare the analysis of the result considering the incoherence and the result not considering the incoherence. Figure 15 and Figure 16 shows the horizontal direction variance.

Looking at the horizontal response of the auxiliary building according to the seismic wave incoherence, the result taking seismic wave incoherence into account shows decreased than the result not



considering seismic wave incoherence. This decrease is prominent in a high-frequency range ( $10\text{Hz} \leq$ ). Comparing the variance based on each seismic load, the structure response of UHS wave is vastly decreased compared to that of RG 1.60 wave, and the variance difference per seismic load is minimal in the low-frequency range ( $>10\text{Hz}$ ) while it is largely decreased in a high-frequency range. Such a result demonstrates that the overall size of the subject model used for analysis is large and well reflects the seismic wave incoherency effect, which lowers the response in a high-frequency range. Based on the coherency model, Luco & Mita's model showed more significant decrease than Abrahamson's model.

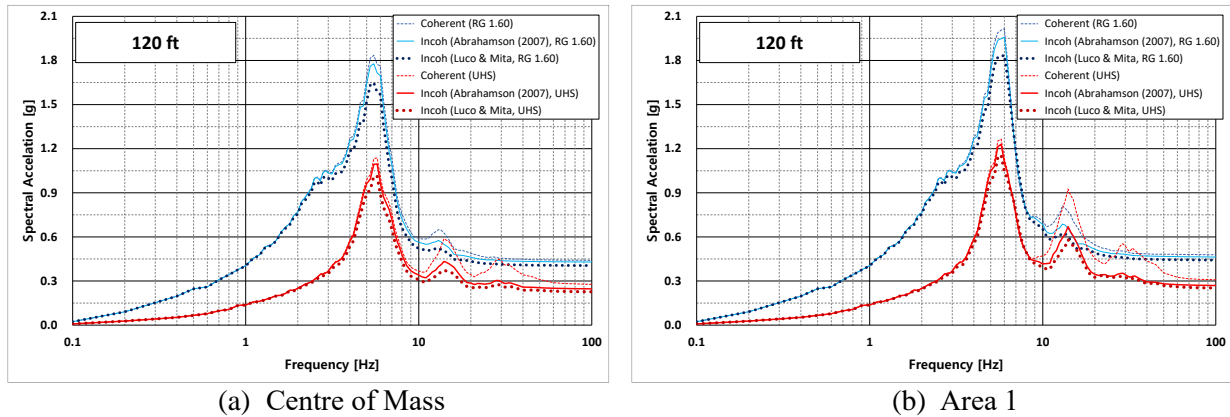


Figure 14. Comparison of ISRS for seismic wave incoherency Effect (Horizontal, 120 ft, Damping 5%)

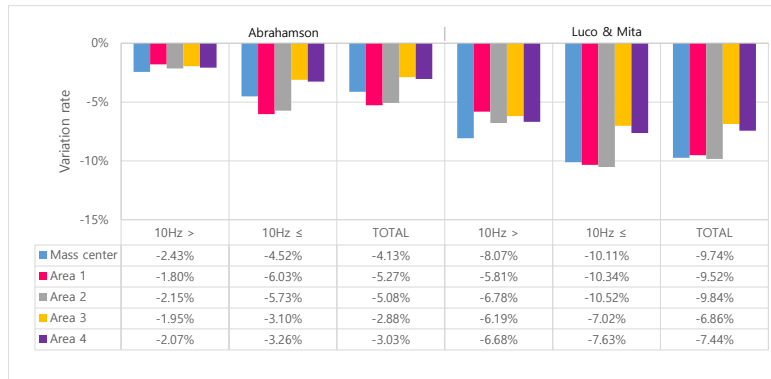


Fig. 15. Comparison of variance for RG 1.60 Wave (Horizontal, 120 ft)

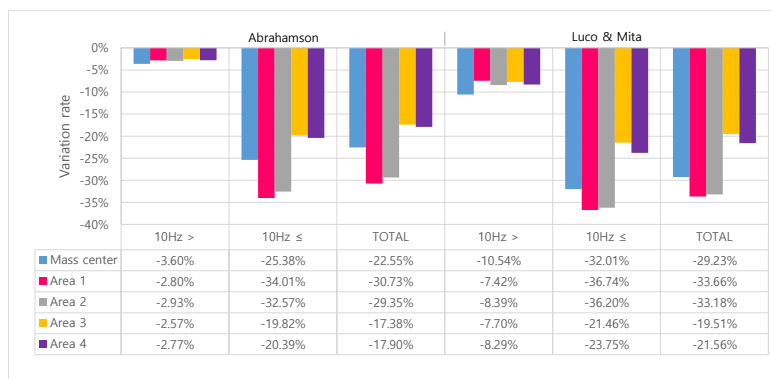


Fig. 16. Comparison of variance for UHS Wave (Horizontal, 120 ft)

## CONCLUSION

This study performed SSI analysis on the auxiliary building to understand the effect of a high-frequency earthquake that exceeds the designed limit on a nuclear power plant and studied the effect of a high-frequency earthquake using seismic waves with two different frequencies. Also, the effect of three-dimensional directional component combinations, change of soil properties, and seismic wave incoherency effect of seismic wave given to a high-frequency earthquake is analyzed. The conclusion is as follows.

In the case of a three-dimensional directional component combination, the response in the outskirts increases more than the auxiliary building's center of mass. Also, it is shown that directional component combination is important because the torsional influence on a structure increases when a high-frequency earthquake is applied.

The result of analyzing the effect of soil properties change on the response of the auxiliary building indicated that the more solid the soil is, the more horizontal and vertical response of RG 1.60 earthquakes, as well as all high-frequency earthquakes, increases overall.

When taking the seismic wave incoherency effect of a seismic wave into account, the auxiliary building's overall horizontal response decreased, and a high-frequency range of 10Hz or more in a high-frequency earthquake showed a large response decrease.

## ACKNOWLEDGMENTS

This work was supported by the Korea Institute of Energy Technology Evaluation and Planning (KETEP) and the Ministry of Trade, Industry & Energy (MOTIE) of the Republic of Korea (No. 20171510101910).

## REFERENCES

- Abrahamson, N.A., (2007), "Hard Rock Coherency Functions Based on the Pinyon Flat Data", *Electric Power Research Institute*, EPRI and US Department of Energy
- Luco, J. E. and A. Mita (1987), "Response of Circular Foundation to Spatially Random Ground Motion" *Journal of Engineering Mechanics*, *Journal of Engineering Mechanics*, ASCE, Vol. 113, No. 1. 1-15
- REGULATORY GUIDE 1.60, (2014), "Design Response Spectra for Seismic Design of Nuclear Power Plants", US-NRC, Rev. 2
- Standard Review Plan 3.7.2, (2013), "SEISMIC SYSTEM ANALYSIS", U.S. Nuclear Regulatory Commission, NUREG, Rev.4

Table 1: Abrahamson's hard rock model coefficients

	Horizontal Coefficient	Vertical Coefficient
$a_1$	1.0	1.0
$a_2$	40	200
$a_3$	0.4	0.4
$n_1(\xi)$	$3.8 - 0.04 \times \ln(\xi + 1) + 0.0105 \times \{\ln(\xi + 1) - 3.6\}^2$	$2.03 - 0.41 \times \ln(\xi + 1) + 0.078 \times \{\ln(\xi + 1) - 3.6\}^2$
$n_2$	16.4	10
$f_c(\xi)$	$27.9 - 4.82 \times \ln(\xi + 1) + 1.24 \times \{\ln(\xi + 1) - 3.6\}^2$	$29.2 - 5.2 \times \ln(\xi + 1) + 1.45 \times \{\ln(\xi + 1) - 3.6\}^2$